STATE OF THE CLIMATE IN 2019

Special Supplement to the
Bulletin of the American Meteorological Society
Vol. 101, No. 8, August 2020

STATE OF THE CLIMATE IN 2019

THE TROPICS

H. J. Diamond and C. J. Schreck, Eds.

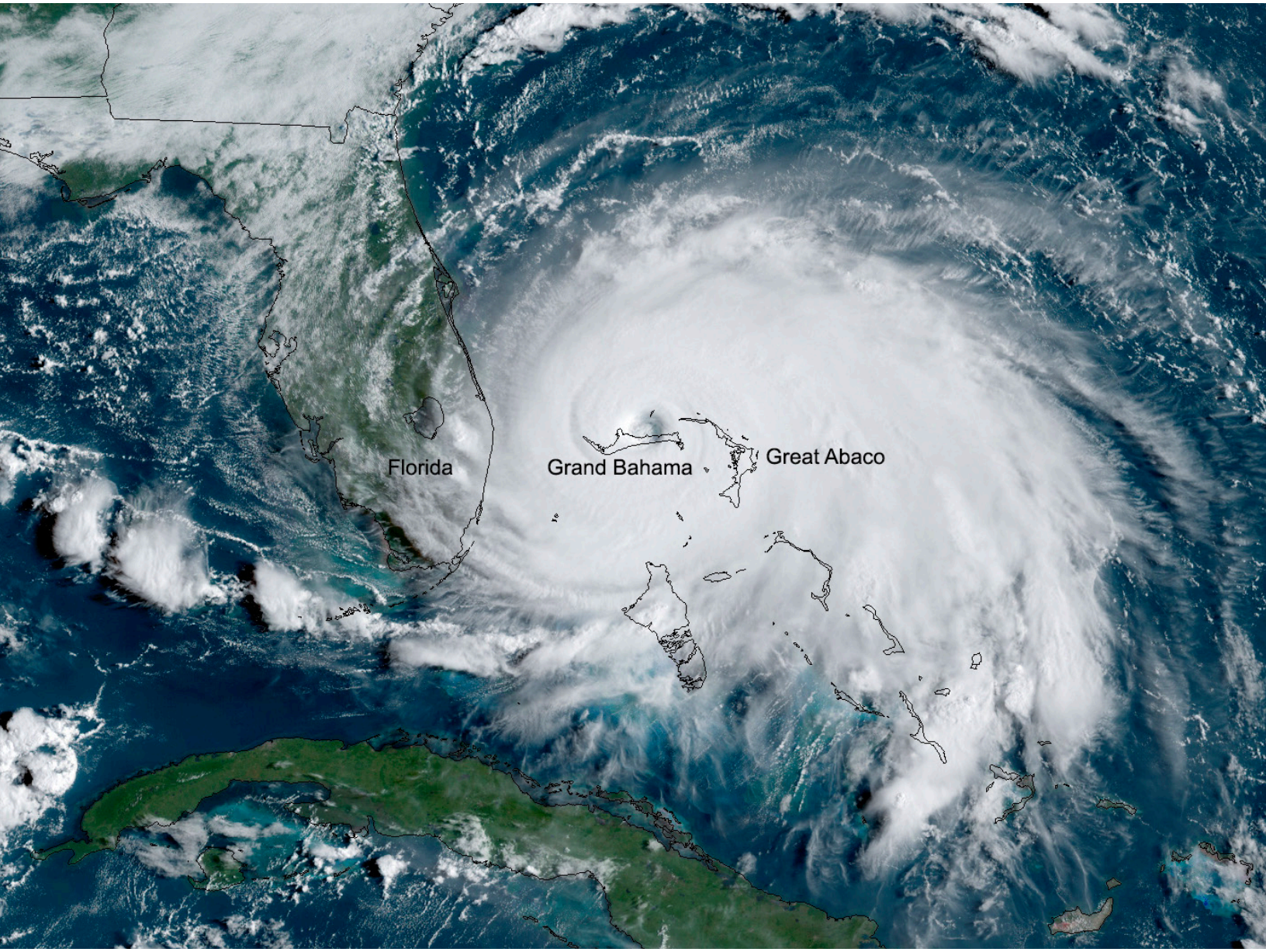

Special Online Supplement to the *Bulletin of the American Meteorological Society,* Vol.101, No. 8, August, 2020

https://doi.org/10.1175/BAMS-D-20-0077.1
Corresponding author: Howard J. Diamond / howard.diamond@noaa.gov

STATE OF THE CLIMATE IN 2019
The Tropics

Editors

Jessica Blunden
Derek S. Arndt

Chapter Editors

Peter Bissolli
Howard J. Diamond
Matthew L. Druckenmiller
Robert J. H. Dunn
Catherine Ganter
Nadine Gobron
Rick Lumpkin
Jacqueline A. Richter-Menge
Tim Li
Ademe Mekonnen
Ahira Sánchez-Lugo
Ted A. Scambos
Carl J. Schreck III
Sharon Stammerjohn
Diane M. Stanitski
Kate M. Willett

Technical Editor

Andrea Andersen

BAMS Special Editor for Climate

Richard Rosen

American Meteorological Society

Thousands of people there were left without power while flooding made some roads impassable. Agriculture in New Caledonia was significantly affected, and the French government released $1.43 million (U.S. dollars) for recovery. Queensland was hit by large swells for about one week, causing significant beach erosion. More than 30 people required rescue, with some hospitalized, due to turbulent waters. One person drowned just off North Stradbroke Island. Heavy winds also damaged Cavendish banana plantations in Cudgen, New South Wales.

Severe TC Pola began as a tropical disturbance that formed northeast of Tonga on 23 February. Pola intensified into a TD while moving slowly southward. Pola became a Category 1 TC on 26 February and intensified into a Category 2 TC later that day. On 27 February, the system became a severe TC. On 28 February, Pola reached its peak intensity as a Category 4 TC with 10-minute sustained winds of 89 kt (46 m s^{-1}) and a minimum central pressure of 950 hPa.

Severe TC Trevor originated as a tropical low which formed off of the east coast of Papua New Guinea on 15 March. The system tracked southeast, crossing Papua New Guinea south of Port Moresby on 16 March. On 19 March, Trevor made landfall on the far northeast of the Queensland coast as a Category 3 severe TC and crossed Cape York Peninsula, downgrading to a Category 1 storm as it did so. As TC Trevor tracked southwest across the Gulf of Carpentaria, it intensified rapidly to a Category 4 system and then made landfall on the Northern Territory's Gulf coastline east of Borroloola on 23 March. The storm weakened as it moved inland. TC Trevor's peak 10-minute sustained winds were 94 kt (49 m s^{-1}), and its minimum central pressure was 950 hPa. Flooding in Queensland associated with the cyclone caused a farm to suffer loss of cattle and damage to equipment estimated to cost at least $710 000 (U.S. dollars). There was little reported in terms of major damage or injuries in the Northern Territory.

TC Ann originated from a tropical low that formed on 7 May, east of Honiara in the Solomon Islands. The low tracked slowly toward the southwest in a favorable environment, passing close to Honiara on 8 May and then moved southward, passing between the Australian cyclone region and South Pacific cyclone region three times over several days. On 11 May, the system intensified into a Category 1 TC before turning west-northwest and further strengthening over the Coral Sea. On 12 May, Ann reached peak intensity as a Category 2 TC with 10-minute sustained winds of 51 kt (26 m s^{-1}) and a central barometric pressure of 993 hPa. TC Ann weakened to a gale-force tropical low on 14 May and made landfall near Lockhart River on Cape York Peninsula on 15 May. The system continued to track west-northwest for several days and dissipated as a tropical low near East Timor on 18 May. Impacts associated with TC Ann were relatively minor, with heavy rainfall and gusts experienced in many areas south of where the system made landfall as a tropical low.

g. Tropical cyclone heat potential—R. Domingues, G. J. Goni, J. A. Knaff, I-I Lin, and F. Bringas

Upper-ocean thermal conditions observed during 2019 within the seven tropical cyclone (TC) basins are described here with respect to the long-term mean (1993–2018) and to conditions observed in 2018. The analysis focuses on vertically integrated temperature conditions based on the Tropical Cyclone Heat Potential (TCHP; e.g., Goni et al. 2009, 2017) which is calculated as the integrated heat content between the sea surface and the depth of the 26°C isotherm (the minimum temperature required for genesis and intensification, Leipper and Volgenau 1972; Dare and McBride 2011). The TCHP is an indicator of the amount of heat stored in the upper ocean and available to fuel TC intensification and modulates TC-induced sea surface temperature (SST) cooling and ocean–hurricane enthalpy fluxes (e.g., Lin et al. 2013). Areas in the ocean with TCHP values above 50 kJ cm^{-2} have been associated with TC intensification and rapid intensification (e.g., Shay et al. 2000; Mainelli et al. 2008; Lin et al. 2014; Knaff et al. 2018), provided that atmospheric conditions are also favorable. Salinity in the upper layers also modulates upper-ocean turbulent mixing and, thus, can also impact the depth of the 26°C isotherm and the corresponding TCHP values (e.g., Balaguru et al. 2015; Domingues et al. 2015).

The analysis developed here focuses primarily on seasonal TCHP anomalies (Fig. 4.36) calculated as departures from the long-term mean (1993–2019) for the primary months of TC activity in each hemisphere: June–November 2019 in the Northern Hemisphere (NH) and November 2018–April 2019 in the Southern Hemisphere (SH). Differences between the 2019 and 2018 seasons are also analyzed (Fig. 4.37). In any given TC basin, TCHP anomalies can exhibit large spatial and temporal variability linked with large mesoscale ocean features, and short-term, interannual (e.g., El Niño-Southern Oscillation [ENSO]), and longer-term ocean variability, such as the Pacific Decadal Variability.

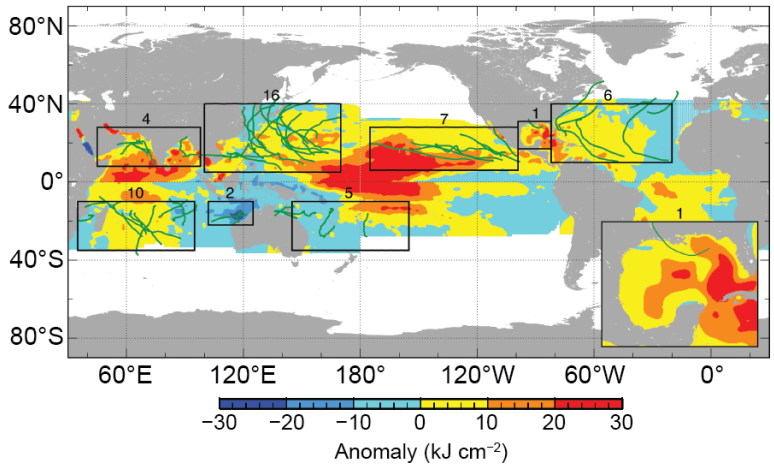

Fig. 4.36. Global anomalies of TCHP during 2019 computed as described in the text. Boxes indicate the seven regions where TCs occur: from left to right, Southwest Indian, North Indian, West North Pacific, Southeast Indian, South Pacific, East Pacific, and North Atlantic (shown as Gulf of Mexico and tropical Atlantic separately). The green lines indicate the trajectories of all TCs reaching at least Category-1 (1-min average wind ≥ 64 kts, 34 m s^{-1}) and above during Nov 2018–Apr 2019 in the SH and Jun–Nov 2019 in the NH. The numbers above each box correspond to the number of Category-1 and above cyclones that travel within each box. The Gulf of Mexico conditions are shown in the inset in the lower right corner.

The 2019 TC season exhibited above-normal TCHP anomalies, which are favorable for TC development and intensification, in most TC basins (Fig. 4.36). TCHP values also increased in most basins from 2018 to 2019 (Fig. 4.37), with notable warming of 20 kJ cm^{-2} with respect to 2018 observed at: (1) portions of the Gulf of Mexico associated with Loop Current dynamics; (2) large areas in the South and North Indian Ocean basins; and (3) the western North Pacific basin Main Development Region (MDR; Lin et al. 2014), i.e., east of the Philippines between 5°N and 20°N, and 100°–170°E. Negative TCHP anomalies with respect to long-term conditions (Fig. 4.36) and the 2018 season (Fig. 4.37) were only observed in the southeast Indian basin and near the eastern portion of the South Pacific basin.

Both the North and southwest Indian Ocean basins exhibited considerably large TCHP values in 2019 (Fig. 4.36), with anomalies as large as ~30 kJ cm^{-2} larger than the long-term average in most of the North Indian basin, including the Bay of Bengal and Arabian Sea; and ~20 kJ cm^{-2} in the southeast Indian basin. In particular, TCHP values were consistently larger than 90 kJ cm^{-2} in the North Indian basin and 70 kJ cm^{-2} in the southeast basin (not shown). Consistent with these substantially warmer conditions, both the North and southwest Indian basins were characterized by above-normal TC activity. In the North Indian basin, the 2019 TC season was one of the most active on record (see section 4f5; Fig. 4.36). In the southwest Indian basin, the 2019 TC season was the most active, costliest, and deadliest on record (see section 4f6).

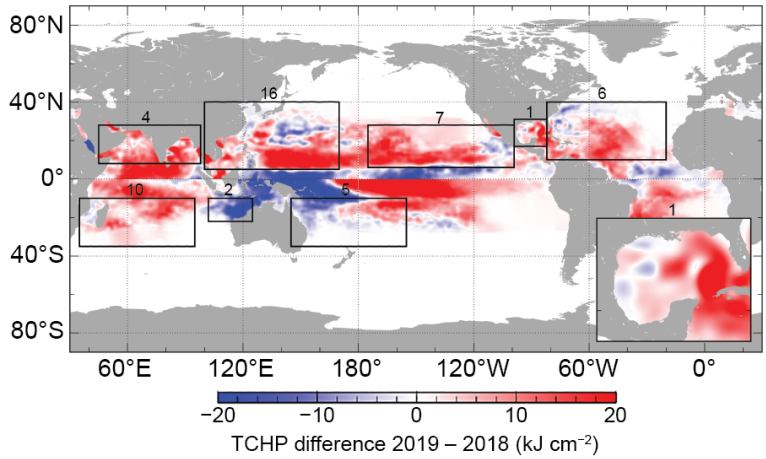

Fig. 4.37. TCHP difference between the 2019 and 2018 tropical cyclone seasons (Jun–Nov in the NH and Nov–Apr in the SH).

In the North Pacific, upper-ocean thermal conditions are largely modulated by the state of ENSO (e.g., Lin et al. 2014, 2020; Zheng et al. 2015), which can impact conditions both in the western and eastern North Pacific basins. During

the 2019 TC season, ENSO conditions switched from neutral in late 2018 to a weak El Niño in early 2019 and back to neutral conditions by mid-2019. Associated with the neutral ENSO state, the MDR within the western North Pacific basin exhibited TCHP values approximately 10–20 kJ cm^{-2} larger than the long-term mean (Fig. 4.36) and ~20 kJ cm^{-2} larger than 2018 conditions (Fig. 4.37). These anomalies led to absolute TCHP values of 120 kJ cm^{-2} or larger over the MDR and of at least 70 kJ cm^{-2} over most of this basin. Among the TCs that formed in this basin, Super Typhoon Hagibis was a notable TC that experienced rapid intensification while traveling over areas with TCHP of 100 kJ cm^{-2} or larger, where it became Category 5 (not shown). Another notable case is Super Typhoon Halong, which also rapidly intensified over the MDR in areas with large TCHP values (~100 kJ cm^{-2}) in November, reaching a maximum wind speed of 155 kts (80 m s^{-1}). Halong was the most intense TC globally in 2019, but fortunately did not make landfall.

In the eastern North Pacific basin, TCHP values were consistently larger than long-term average conditions by 10–30 kJ cm^{-2} (Fig. 4.36). Compared to 2018 conditions, TCHP values were ~20 kJ cm^{-2} larger in 2019 over the central part of the basin between 180°W and 120°W and slightly cooler by less than 10 kJ cm^{-2} closer to Central America. Of note, Major Hurricane Erick's rapid intensification west of 140°E was aided by the higher TCHP in this region.

Finally, in the North Atlantic basin, TCHP values were ~10 kJ cm^{-2} above the long-term average (Fig. 4.36) in most parts of the basin, and warmer than 2018 in the central part of the basin between 60°W and 30°W and in the Gulf of Mexico, where the Loop Current extended northward and shed a warm core ring. Associated with these conditions, the North Atlantic basin exhibited above-normal hurricane activity for the fourth consecutive year. Higher TCHP values over the central portion of the basin likely contributed to the rapid intensification of five of the total six hurricanes that developed in that region of the North Atlantic in 2019 (Fig. 4.36). Hurricane Dorian, now regarded as the most powerful hurricane on record for the Atlantic outside of the tropics (>23.5°N) in the satellite era (since 1966), reached its peak intensity while traveling over areas with TCHP values consistently above 70 kJ cm^{-2} and as large as 90 kJ cm^{-2} (not shown). These conditions are well above the 50 kJ cm^{-2} minimum threshold required to support Atlantic hurricane intensification (Mainelli et al. 2008). In addition to high TCHP values, Dorian traveled and intensified over areas with low surface salinity values associated with the Amazon and Orinoco riverine plumes (not shown). Areas with this type of low surface salinity are known for favoring TC intensification by creating barrier layer conditions that suppress upper-ocean mixing, maintaining enthalpy fluxes from the ocean into the hurricane (e.g., Balaguru et al. 2015; Domingues et al. 2015).

In summary, upper-ocean conditions conducive for TC development and intensification observed in 2019 were associated with higher-than-normal values of TCHP in most TC basins in 2019. Notable warming with respect to 2018 was also recorded in most basins, especially in the Gulf of Mexico, the west North Pacific, and the Indian Ocean, particularly the Arabian Sea. These warmer-than-usual conditions contributed to the more intense and above-normal TC activity in most of these basins.

h. Indian Ocean dipole—L. Chen, J.-J. Luo, and A.D. Magee

The Indian Ocean dipole (IOD) is an inherent air–sea coupling mode in the tropical Indian Ocean. It originates from local air–sea interaction in the Indian Ocean and/or the forcing associated with the El Niño–Southern Oscillation (ENSO) in the tropical Pacific (Saji et al. 1999; Luo et al. 2010). Typically, IOD events develop in boreal summer, peak in boreal autumn, and terminate rapidly in early boreal winter. During the late boreal spring to autumn 2019, a positive IOD (pIOD) with extreme intensity occurred for the first time since 1997. Prior to the pIOD event in 1997, the previous extreme pIOD event occurred in 1994 (Luo et al. 2007, 2008).

In the tropical Pacific, a weak El Niño occurred in the boreal winter of 2018/19 and returned to neutral conditions by the boreal summer of 2019, but the sea surface anomalously warmed there during the autumn of 2019 (Fig. 4.38c). In the tropical Indian Ocean, a weak pIOD occurred during